Analysis of acoustic transmission for one directional periodic bounded structure in 2D by BEM

Haifeng GAO[1)], Toshiro MATSUMOTO[2)], Toru TAKAHASHI[3)], Hiroshi ISAKARI[4)]

1)Nagoya University (Furo-cho, Chikusa-ku, Nagoya, 464-8603, Japan, E-mail: gao_h@nuem.nagoya-u.ac.jp)
2)Nagoya University (Furo-cho, Chikusa-ku, Nagoya, 464-8603, Japan, E-mail: t.matsumoto@nuem.nagoya-u.ac.jp)
3)Nagoya University (Furo-cho, Chikusa-ku, Nagoya, 464-8603, Japan, E-mail: ttaka@nuem.nagoya-u.ac.jp)
4)Nagoya University (Furo-cho, Chikusa-ku, Nagoya, 464-8603, Japan, E-mail: isakari@nuem.nagoya-u.ac.jp)

In this paper, the acoustic transmission of one directional 2D finite periodic bounded structure is investigated by BEM, and to avoid solving the whole matrix, a size-reduced system matrix is formulated to compute the transmission problem. In the size-reduced system matrix, the unknowns on free boundary of the periodic parts are removed. Also the block Sakurai-Sugiura (SS) method is employed to compute the band structure of a unit cell for the infinite periodic structure. In order to eliminate the fictitious eigenvalues resulted by internal closed boundary, Burton-Miller's method is used. Furthermore, we compute the eigenfrequencies of the finite structure having periodic parts and show that the distribution of the eigenfrequencies follows the location of bandgap. Numerical results show that when the number of layers of the periodic parts in the finite periodic structure is large enough, the transmissivity is in a good agreement with the bandgaps.

Key Words: finite periodic structure, block Sakurai-Sugiura Method, eigenfrequency, boundary element method

1. Introduction

The studies of 1D periodic structures or materials have received considerable attention in the literature[1, 2, 3, 4]. Due to the dispersive nature of periodic structures, they may exhibit frequency range where the propagation of mechanical waves are forbidden. These frequency ranges are commonly called stop bands or bandgaps and the remaining ranges are called pass bands. To compute the dispersion curves and find the bandgaps, transfer matrix method[2, 3, 4] is often used, however boundary element method (BEM) is also an attractive method to find bandgaps since it can keep the unknowns on the boundary where homogenous boundary condition is given.

Block SS method[5, 6, 7, 8, 9, 10], which is one of contour integral methods, converts the nonlinear eigenvalue problem (NEP) to a generalized eigenvalue problem of two Hankel matrices with a reduced eigenspace. The dimension of the Hankel matrices is very small and computational cost is neglectable comparing with the original system matrix. The main computational cost is, however, the evaluation of the moment matrices which are used to form the Hankel matrices. It results in solving BEM for N times which is the number of points on the contour integral path when trapezoidal rule is employed. The emerging of fast algorithm such as fast multipole boundary element method (FMBEM)[11], adaptive cross-approximation boundary element method (ACA-BEM)[12, 13] makes it possible to solve eigenvalue problem by using BEM efficiently.

We presented eigenvalue analysis for 2D cavities, in author's previous research[14], in which only simply connected region is considered, so there is no internal closed boundary or fictitious eigenvalues exist in the numerical results.

In this research, we apply the block SS method to compute the eigenvalues of the transmission problems in one directional periodic bounded structure in two dimensional domain. To reduce the dimension of the system matrix, we only carry out the integration of unit cell once and represent the unknowns on the free boundary by using the unknowns on connection interfaces which are considered as virtual interfaces if the same materials are used at the connection interfaces of adjacent cells, but if the materials are not same, then the interfaces are not virtual. For the calculation of dispersion curves, the scatter in the matrix material has a closed boundary which means that the domain is a complex connected region. The internal closed boundary results in appearance of fictitious eigenvalues when the eigenvalue problem is solved by using block SS method with conventional BEM. In order to acquire the correct results without any fictitious eigenvalues, we here employ Burton-Miller's method [15], by which large imaginary components are added to the fictitious eigenvalues, then they can be filtered because of the large imaginary part. Numerical examples with the different number of finite periodic layers are given to demonstrate the correctness of proposed methodology.

2. Formulation

In physics, the propagation of acoustic waves through a material medium is governed by the Helmholtz euqation:

$$\nabla^2 p(x) + k^2 p(x) = 0 \quad \text{in } T, \tag{1}$$

Received Sep. 28, 2012, accepted Nov. 8, 2012

where p is the sound pressure, ∇^2 is the Laplace operator, and $k = \frac{\omega}{C}$ is a predefined wave number, ω is circular frequency, C is the wave speed, and T is the domain. Usually we have the following boundary conditions:

$$p = \bar{p} \quad \text{on } S_p,$$
$$q = \frac{\partial \bar{p}}{\partial n} = \mathrm{i}\rho\omega\bar{v} \quad \text{on } S_q,$$

where n is the normal direction at the boundary, ρ is the density, v is the particle velocity.

Equation (1) can be transformed into the integral equation by using the following fundamental solution (2) and its normal derivative (3) for 2D Helmholtz equation:

$$p^*(x,y) = \frac{\mathrm{i}}{4}H_0^{(1)}(kr), \tag{2}$$

$$q^*(x,y) = \frac{\partial p^*(x,y)}{\partial n(x)} = -\frac{k\mathrm{i}}{4}H_1^{(1)}(kr)\frac{\partial r}{\partial n(x)}, \tag{3}$$

where y is the collocation point and x is the source point, r is the distance between x and y, i is the imaginary unit, $H_i^{(1)}$ denotes the Hankel function of the first kind, $n(x)$ is the outward normal direction to the boundary at x. With Green's identity, the integral representation for $p(y)$ can be obtained as

$$p(y) + \int_S q^*(x,y)p(x)dS(x) = \int_S p^*(x,y)q(x)dS(x). \tag{4}$$

The normal directional derivative of Eq.(4) at y is written as

$$q(y) + \int_S \hat{q}^*(x,y)p(x)\mathrm{d}S(x) - \int_S \hat{p}^*(x,y)q(x)\mathrm{d}S(x) = 0 \quad \text{in } T, \tag{5}$$

where $\hat{p}^*(x,y)$ and $\hat{q}^*(x,y)$ are the normal directional derivative of $p^*(x,y)$ and $q^*(x,y)$, respectively:

$$\hat{p}^*(x,y) = \frac{\partial p^*(x,y)}{\partial n(y)} = -\frac{k\mathrm{i}}{4}H_1^{(1)}(kr)\frac{\partial r}{\partial n(y)}, \tag{6}$$

$$\begin{aligned}\hat{q}^*(x,y) &= \frac{\partial q^*(x,y)}{\partial n(y)} \\ &= -\frac{k^2\mathrm{i}}{8}[H_0^{(1)}(kr) - H_2^{(1)}(kr)]\frac{\partial r}{\partial n(y)}\frac{\partial r}{\partial n(x)} \\ &\quad -\frac{k\mathrm{i}}{4}H_1^{(1)}(kr)\frac{\partial^2 r}{\partial n(y)\partial n(x)}.\end{aligned} \tag{7}$$

Let the internal point y tend to the boundary of T, then, evaluating the boundary integrals in Eqs. (4) and (5), we obtain the following boundary integral equaitons:

$$c_y p(y) + \oint_S q^*(x,y)p(x)dS(x) = \int_S p^*(x,y)q(x)dS(x), \tag{8}$$

$$c_y q(y) + \oint\!\!\!\!\!\!= \int_S \hat{q}^*(x,y)p(x)\mathrm{d}S(x) = \oint\!\!\!\!\!\!= \int_S \hat{p}^*(x,y)q(x)\mathrm{d}S(x), \tag{9}$$

where $c_y = \frac{1}{2}$ if S is smooth around y, $\oint$ denotes that the integral must be evaluated in the sense of Cauchy's principal value, $\oint\!\!\!\!\!\!=$ denotes that the integral must be evaluated in the sense of finite-part value of divergent integral.

Let us consider two domains connected by a certain number of periodic structures shown in Fig.1, in which Ω_i denotes the input domain, Ω_o denotes the output domain, $D_1, D_2, \cdots, D_n$ are the matrix domains of the periodic parts, $\Sigma_1, \Sigma_2, \cdots, \Sigma_n$ are scatters in the corresponding matrix domains.

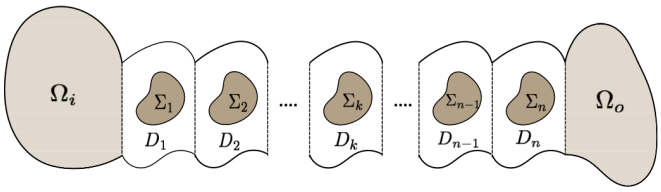

Fig. 1 The finite periodic structure.

First, let us derive the system equations of a unit cell in the periodic parts. In Fig.2, the boundary of the l-th cell is defined as follows: the boundary shown with a broken line on the left-hand side is the output boundary Γ_o^{l-1} of cell $l-1$ and also the input boundary Γ_i^l of cell l; similarly, the boundary shown with a broken line on the right-hand side is the output boundary Γ_o^l of cell l and also the input boundary Γ_i^{l+1} of cell $l+1$. Γ_s^l denotes the remaining free part of the boundary.

The discretized boundary integral equations of a unit cell can be written in a matrices form as follows:

$$\begin{pmatrix} H_{ii} & H_{io} & H_{is} \\ H_{oi} & H_{oo} & H_{os} \\ H_{si} & H_{so} & H_{ss} \end{pmatrix}\begin{pmatrix} p_i \\ p_o \\ p_s \end{pmatrix} = \begin{pmatrix} G_{ii} & G_{io} & G_{is} \\ G_{oi} & G_{oo} & G_{os} \\ G_{si} & G_{so} & G_{ss} \end{pmatrix}\begin{pmatrix} q_i \\ q_o \\ q_s \end{pmatrix}. \tag{10}$$

In Eq.(10), p_i, p_o, p_s, and q_i, q_o, q_s are the sound pressures and its normal derivatives on the input boundary Γ_i, the output boundary Γ_o, and the free boundary Γ_s, respectively.

Rearranging the coefficients of the quantities on the free boundary yields

$$\begin{pmatrix} H_{ii} & H_{io} & A_{is} \\ H_{oi} & H_{oo} & A_{os} \\ H_{si} & H_{so} & A_{ss} \end{pmatrix}\begin{pmatrix} p_i \\ p_o \\ x_s \end{pmatrix} = \begin{pmatrix} G_{ii} & G_{io} & B_{is} \\ G_{oi} & G_{oo} & B_{os} \\ G_{si} & G_{so} & B_{ss} \end{pmatrix}\begin{pmatrix} q_i \\ q_o \\ y_s \end{pmatrix}, \tag{11}$$

where x_s denotes the unknowns, y_s denotes the knowns on the free boundary. Then, x_s can be represented by other quantities, as follows:

$$\begin{aligned}x_s = &-A_{ss}^{-1}H_{si}p_i - A_{ss}^{-1}H_{so}p_o \\ &+A_{ss}^{-1}G_{si}q_i + A_{ss}^{-1}G_{so}q_o + A_{ss}^{-1}B_{ss}y_s.\end{aligned} \tag{12}$$

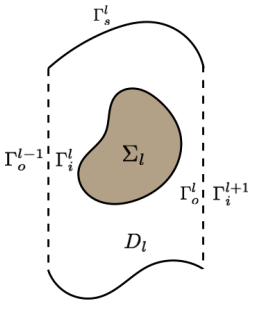

Fig. 2 A unit cell.

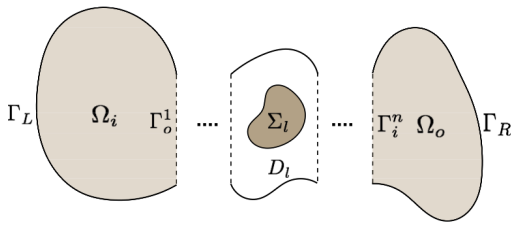

Fig.3 The definition of the boundary of input and output domains.

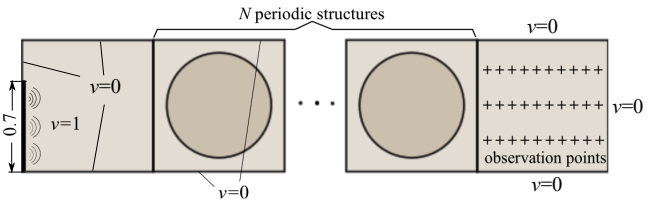

Fig.4 Input and output domains connected by square cells. The cross symbols denote the observation points.

In light of (11) and (12), the unknowns on the free boundary are eliminated, as follows:

$$\begin{pmatrix} H_{io}-A_{is}A_{ss}^{-1}H_{so} & -G_{io}+A_{is}A_{ss}^{-1}G_{so} \\ H_{oo}-A_{os}A_{ss}^{-1}H_{so} & -G_{oo}+A_{os}A_{ss}^{-1}G_{so} \end{pmatrix} \begin{pmatrix} p_o \\ q_o \end{pmatrix} = \begin{pmatrix} -H_{ii}+A_{is}A_{ss}^{-1}H_{si} & G_{ii}-A_{is}A_{ss}^{-1}G_{si} \\ -H_{oi}+A_{os}A_{ss}^{-1}H_{si} & G_{oi}-A_{os}A_{ss}^{-1}G_{si} \end{pmatrix} \begin{pmatrix} p_i \\ q_i \end{pmatrix} + \begin{pmatrix} B_{is}-A_{is}A_{ss}^{-1}B_{ss} \\ B_{os}-A_{os}A_{ss}^{-1}B_{ss} \end{pmatrix} \begin{pmatrix} y_s \end{pmatrix}. \quad (13)$$

Let the coefficient matrices in Eq.(13) be represented by M, N, Ly_s respectively, then Eq.(13) can be written in a more compact form:

$$Mx^{l+1} = Nx^l + Ly_s, \quad (14)$$

where x^l and x^{l+1} denotes the quantities on the input and output boundaries, respectively. It should be noticed that the normal derivatives in x^{l+1} have interior normal direction in Eq.(14). For the input domain Ω_i and output domain Ω_o, their boundaries are defined in Fig.3. The system of the algebraic equations for the input and output domains is written in the following form:

$$A_L x^L + A_{L1} x^1 = y^L, \quad (15)$$

$$A_{Rn} x^n + A_R x^R = y^R, \quad (16)$$

where x^1 denotes the quantities on Γ_o^1, x^L denotes the quantities on Γ_L, x^n denotes the quantities on Γ_i^n, and x^R denotes the quantities on Γ_R.

Combining all the algebraic equations (14), (15), and (16) together, the entire matrix equation in which the unknowns on all the free boundaries are eliminated is obtained as follows:

$$\begin{pmatrix} A_L & A_{L1} & 0 & 0 & 0 & 0 & 0 \\ 0 & -N & M & 0 & 0 & 0 & 0 \\ 0 & 0 & -N & M & 0 & 0 & 0 \\ 0 & 0 & 0 & \ddots & \ddots & 0 & 0 \\ 0 & 0 & 0 & 0 & -N & M & 0 \\ 0 & 0 & 0 & 0 & 0 & A_{Rn} & A_R \end{pmatrix} \begin{pmatrix} x^L \\ x^1 \\ x^2 \\ \vdots \\ x^n \\ x^R \end{pmatrix} = \begin{pmatrix} y^L \\ Ly_s \\ Ly_s \\ \vdots \\ Ly_s \\ y^R \end{pmatrix}. \quad (17)$$

In this formula, we have only three unknown groups: (i) the input domain, (ii) the output domain, (iii) connection interfaces of the cells. All unknowns on the free boundary of the connection parts are removed, for instance, if we consider 100 layers of periodic structure and the number of elements for free boundary of unit cell is 20, then $20 \times 100 = 2000$ unknowns and equations are reduced.

We now consider an infinite one directional 2D periodic structure formed with the cells shown in Fig. 2. Then, the system of the algebraic equations can be written in the form:

$$\begin{bmatrix} H_i & H_o & H_s \end{bmatrix} \begin{bmatrix} p_i \\ p_o \\ p_s \end{bmatrix} = \begin{bmatrix} G_i & G_o & G_s \end{bmatrix} \begin{bmatrix} q_i \\ q_o \\ q_s \end{bmatrix}. \quad (18)$$

According to Bloch's theorem, the following relations hold:

$$p_o = p_i \exp(\mathrm{i}ka), \quad (19)$$

$$q_o = q_i(-\exp(\mathrm{i}ka)), \quad (20)$$

where a is the length of a single cell along the periodic direction, k is the wave vector. When we substitute above relations and the homogenous boundary condition on the free boundary to Eq.(18), we have the following system of NEP:

$$\begin{pmatrix} H_i + H_o \exp(\mathrm{i}ka) & -G_i - G_o(-\exp(\mathrm{i}ka)) & A_s \end{pmatrix} \times \begin{pmatrix} p_i \\ q_i \\ x_s \end{pmatrix} = 0. \quad (21)$$

As $k = \frac{\omega}{C}$, the eigenvalue parameter ω is involved in coefficient matrix of Eq. (21) implicitly. Here, we employ a contour integral method, the block SS method as an eigensolver which has been applied to solve the eigenvalues of a 2D acoustic cavity by BEM [14], and Burton-Miller's method is used to eliminate the fictitious eigenvalues. The parameter α of Burton-Miller's method is chosen as $\mathrm{i}/2k$.

3. Numerical example

A finite structure having periodic parts is depicted in Fig.4. Square input and output domains are connected by N layers of square cells with cylinder scatters, and all sides of the square structures are assumed to be 1[m]. A nonsymmetrical excitation is given as the particle velocity $v = 1[\mathrm{m/s}]$ on 70% of the edge of the input domain, while in the output domain, 30 observation points are distributed. The points from number 1 to 10, 11 to 20 and 21 to 30 have the same y coordinates as $y = 0.5$, $y = 0.25$, $y = 0.75$ respectively, while x coordinates for the each 10 points are 0.05, 0.15, $\cdots$, 0.95, and unit is [m]. First, assuming that the unit cell is one layer of an infinite one directional periodic structure and solving the NEP given

Table 1 Parameters of the model.

Sound velocity [m/s]	337.2
Density [kg/m^3]	1.22
Filling fraction	0.503
Filling material	rigid
Cell length [m]	1

by Eq.(21) using BEM based on Burton-Miller's method, we obtain the dispersion curves corresponding to the variable wave vector k from 0 to π. For the Block SS method, solved range is assumed as [500,4500]. The numerical results for the dispersion curves obtained by the conventional BEM and that based on Burton-Miller's method are shown in Figs.5 and 6, respectively. Since the fictitious eigenvalues are constants when the wave vector k varies from 0 to π, there are horizontal lines showing fictitious eigenvalues in Fig.5.

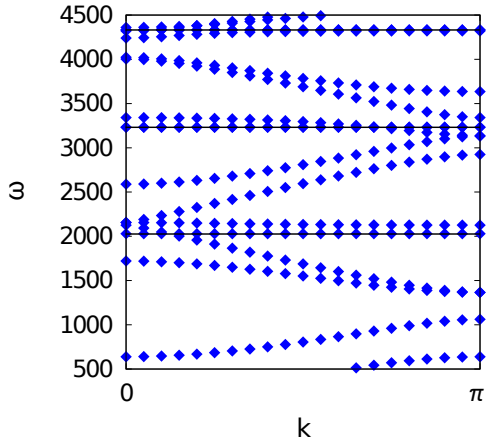

Fig. 5 Dispersion curves (by conventional BEM) with fictitious eigenvalues (horizontal lines).

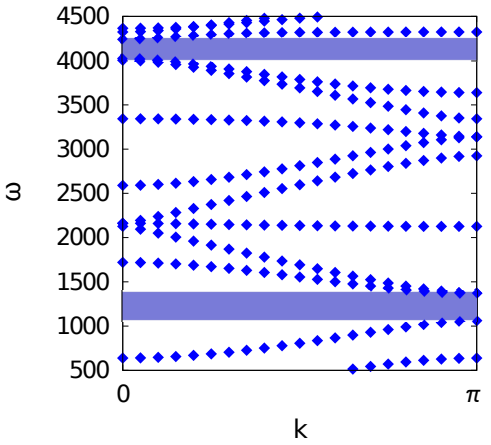

Fig.6 Dispersion curves (by the Burton-Miller method) and bandgaps (shade).

Next, let us consider the transmission problem and use different models by changing the layers of the connection parts. The transmissivities of the finite periodic structure with 12, 25, 50, 100 layers are shown in Figs.7 to 10, in which the sound pressures at 30 observation points are plotted, and in Figs.7(b) to 10(b) are shown their projections on ω-p plane. From the figures of transmissivity, it is found that the transmissivity becomes very low in the bandgaps particularly when the number of the layers is larger than 25.

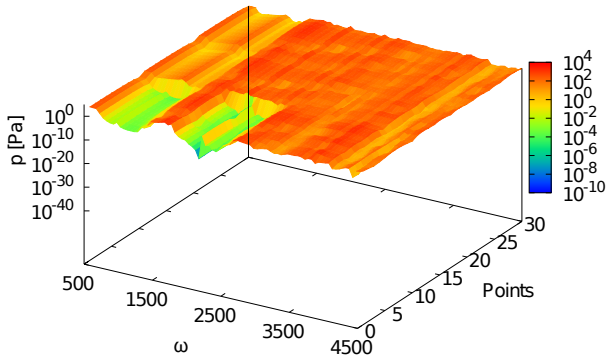

(a)

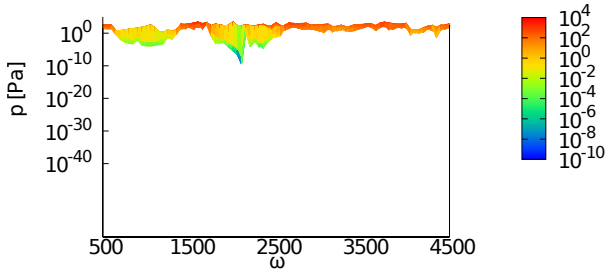

(b)

Fig.7 Transmissivity of finite periodic structure with 12 layers.

To obtain the bandgaps of the finite structure, the block SS method is directly applied to compute the eigenfrequencies of the size-reduced system matrix (17) that is also of a NEP. The eigenfrequencies of models with 12, 25, 50, 100 layers are shown in Figs.11 to 14, respectively, corresponding to the solved range [500,1500] in which 1 bandgap is included. Eigenfrequencies out of this range are also obtained. From these numerical results, it is found that the distribution of the eigenvalues along the real-axis have the bandgap shown in Fig. 6. However, as is found in Figs.11 to 14, two eigenfrequencies 1252.513 and 1262.504 are always found in the range of bandgap. These eigenfrequencies do not change even when the number of layers is changed, hence the two eigenfrequencies can be considered as those corresponding to eigenmodes which have large amplitude in input and output domains while small amplitude in connection part.

4. Conclusion

The present study was undertaken to develop a method for investigations of one directional 2D finite periodic bounded acoustic structures. This was achieved by calculation of transmissivity by solving size-reduced system matrix and bandgap by using BEM combined with the block SS method. By using Bloch's theorem to the unit cell, the block SS method has been directly applied to computation of the NEP formulated by BEM. The fictitious eigen-

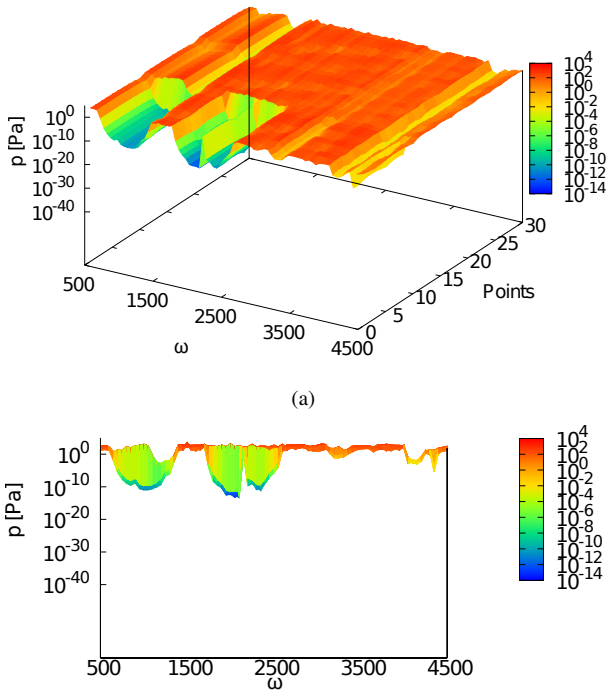

(a)

(b)

Fig. 8 Transmissivity of finite periodic structure with 25 layers.

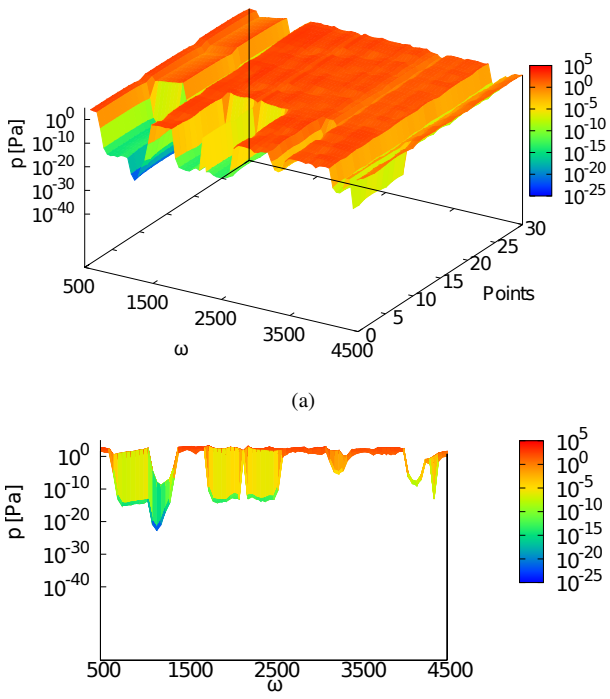

(a)

(b)

Fig. 9 Transmissivity of finite periodic structure with 50 layers.

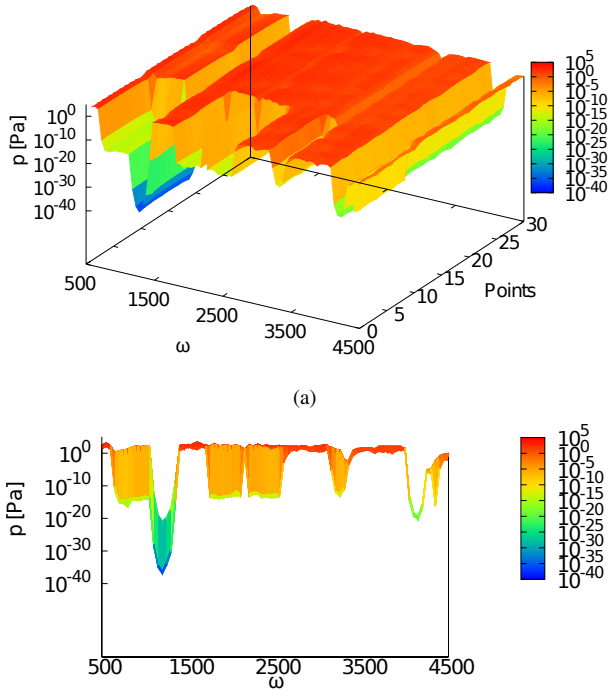

(a)

(b)

Fig. 10 Transmissivity of finite periodic structure with 100 layers.

values observed in the computation could be removed by employing Burton-Miller's method. Furthermore, the eigenfrequencies of the finite periodic bounded structure was also obtained and they showed a bandgap which had a good agreement with the results obtained by computing for the unit cell.

The present work is being further developed to solve the size-reduced matrix by using recursive matrix, because this matrix can be divided into different parts, among which a simple diagonal band matrix is found.

Acknowledgement The authors are grateful to the financial support to this work by JSPS KAKENHI Grant Number 23656121, the China Scholarship Council (CSC), and Nagoya University.

References

(1) E.H. Lee, Wei H. Yang: On waves in composite materials with periodic structure, *J. Comput. Appl. Math.*, **25**, (1973), pp. 492–499.

(2) R. Esquivel-Sirvent, G.H. Cocoletzi: Band-structure for the propagation fo elastic-waves in superlattices, *J. Acoust. Soc. Am.*, **95**, (1994), pp. 86–90.

(3) M.R. Shen, W.W. Cao: Acoustic bandgap formation in a periodic structure with multilayer unit cells, *J. Phys. D-Appl. Phys.*, **33**, (2000), pp. 1150–1154.

(4) M.I. Hussein, G.M. Hulbert, R.A. Scott: Dispersive elastodynamics of 1D banded materials and structures: analysis, *J. Sound Vibr.*, **289**, (2006), pp. 779–806.

(5) T. Sakurai, H. Sugiura: A projection method for generalized eigenvalue problems using numerical integration *J. Comput. Phys.*, **159**, (2003), pp. 119–128.

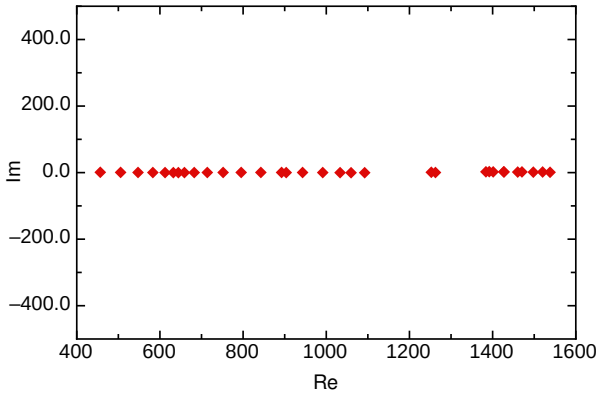

Fig. 11 Eigenfrequencies of finite periodic structure with 12 layers.

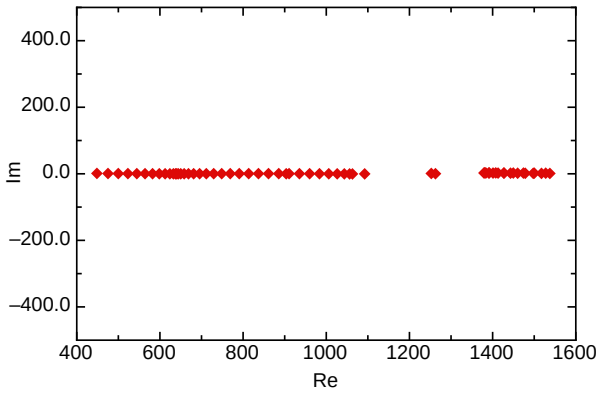

Fig. 12 Eigenfrequencies of finite periodic structure with 25 layers.

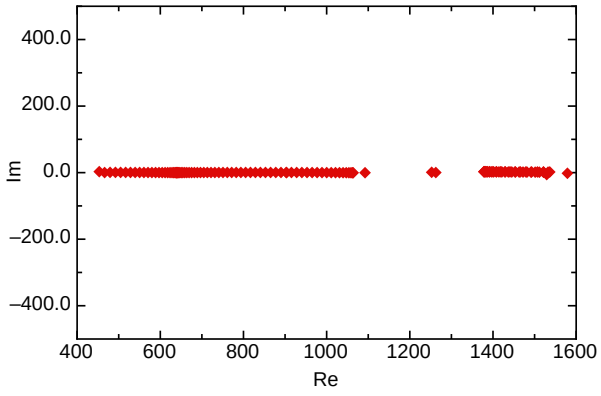

Fig. 13 Eigenfrequencies of finite periodic structure with 50 layers.

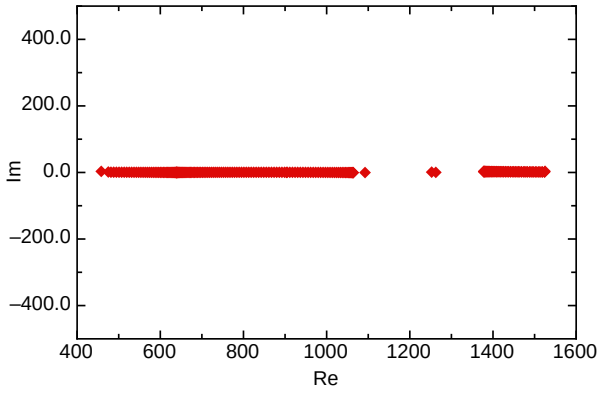

Fig. 14 Eigenfrequencies of finite periodic structure with 100 layers.

(6) T. Ikegami, T. Sakurai, U. Nagashima: A filter diagonalization for generalized eigenvalue problems based on the Sakurai-Sugiura projection method, *J. Comput. Appl. Math.*, **233**, (2010), pp. 1927–1936.

(7) J. Asakura, T. Sakurai, H. Tadano, T. Ikegami, K. Kimura: A numerical method for nonlinear eigenvalue problems using contour integrals, *JSIAM Letters*, **1**, (2009), pp. 52–55.

(8) T. Sakurai, Y. Kodaki, H. Tadano, D. Takahashi, M. Sato, U. Nagashima: A parallel method for large sparse generalized eigenvalue problems using a GridRPC system, *FGCS*, **22**, (2008), pp. 613–619.

(9) T. Sakurai, H. Tadano: CIRR: a Rayleigh-Ritz type method with contour integral for generalized eigenvalue problems, *Hokkaido Math. J.*, **22**, (2008), pp. 613–619.

(10) T. Ikegami, T. Sakurai: Contour integral eigensolver for non-hermitian system: a rayleigh-ritz-type approach, *Taiwan. J. Math.*, **36**, (2007), pp. 745–757.

(11) H. Cheng, W.Y. Crutchfied, Z. Gimbutas, L.F. Greengard, J. Frank Ethridge, J.F. Huang, V. Rokhlin, N. Yarvin, J.S. Zhao: A wideband fast multipole method for the Helmholtz equation in three dimensions, *J. Comput. Phys.*, **216**, (2006), pp. 300–325.

(12) S. Kurz, O. Rain, S. Rjasanow: The adaptive cross-approximation technique for the 3-D boundary-element method, *IEEE Transaction on Magnetics*, **38**, (2002), pp. 421–424.

(13) M. Bebendorf, S. Rjasanow: Adaptive low-rank approximation of collocation matrices, *Computing*, **70**, (2003), pp. 1–24.

(14) H.F. Gao, T. Matsumoto, T. Takahashi, T. Yamada: Eigenvalue analysis for 2D acoustic problem by BEM with SS method, *Transactions of JASCOME*, **11**, (2011), pp. 107–110.

(15) A. J. Bruton, G. F. Miller: The application of integral equation methods to the numerical solution of some exterior boundary-value problems, *Proceedings of the Royal Society of London. Series A*, **323**, (1971), pp. 201–210.